

1a. Shock Tube A Conditions

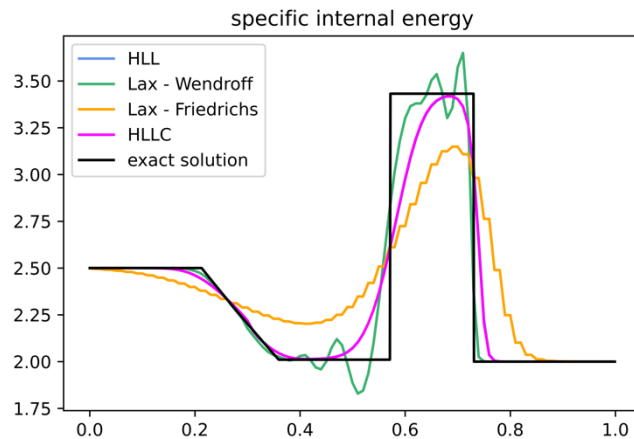


Figure 1: The specific internal energy of the shock tube A system after 0.2s. The different solvers can be seen compared to the exact solution. The HLL and HLLC solvers are very close to each other and hence appear almost super imposed on each other.

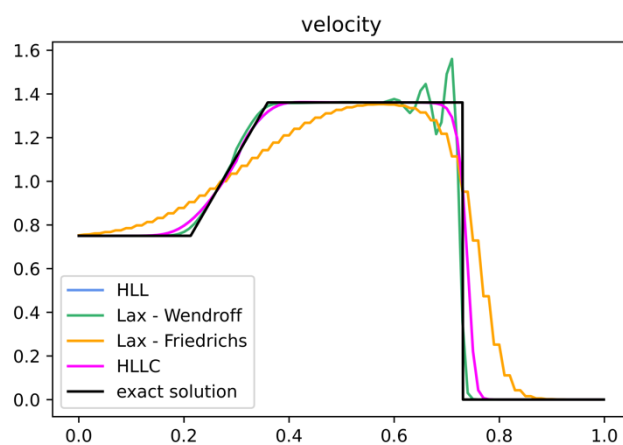


Figure 2: The velocity of the shock tube A system after 0.2s. The different solvers can be seen compared to the exact solution. Again HLL and HLLC solvers achieve almost the same result and hence appear almost super imposed on each other.

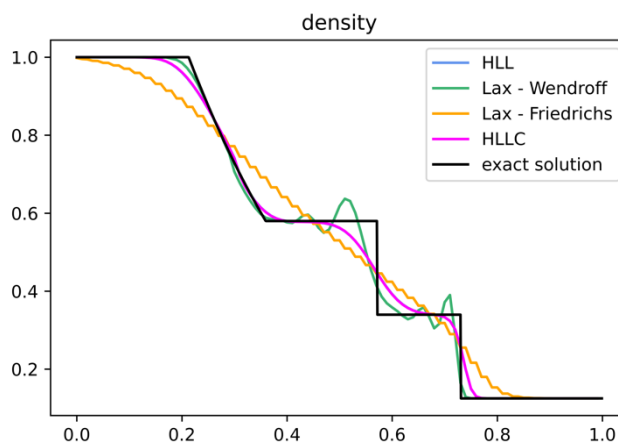


Figure 3: The density of the shock tube A system after 0.2s. The different solvers can be seen compared to the exact solution. Again HLL and HLLC solvers appear almost super imposed on each other due to the similarities in the result.

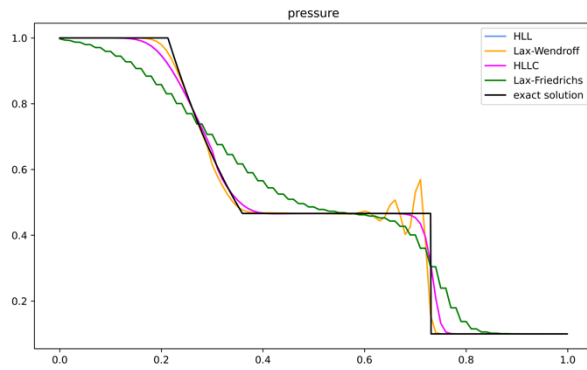
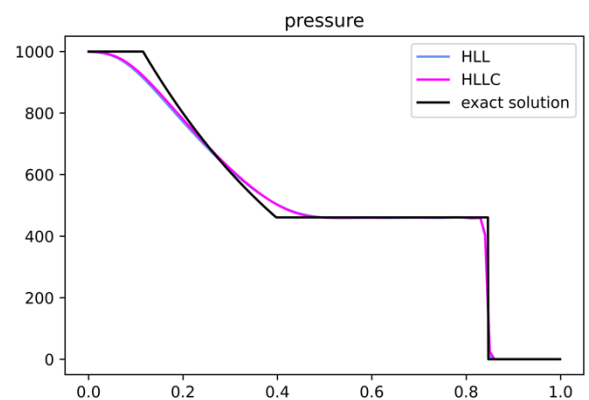
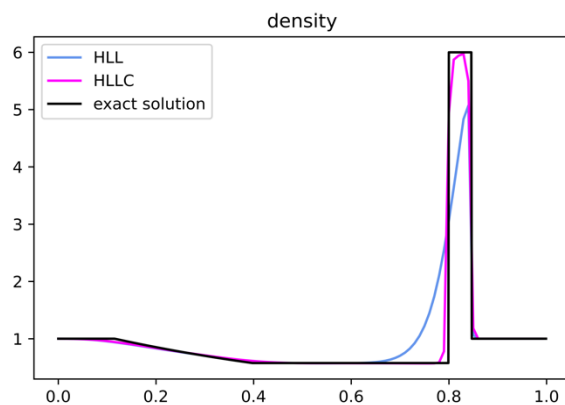


Figure 4: The density of the shock tube A system after 0.2s. The different solvers can be seen compared to the exact solution. Again HLL and HLLC solvers appear super imposed on each other due to the similarities on the data produced.

Four different approaches were taken when investigating this question, each using a different solve. The Lax-Friedrichs solver was used as a baseline, and more advanced solvers in the form of the Lax-Wendroff, HLL and HLLC were compared. It is clear from the graphs above that both the HLL and HLLC method are far superior when compared to their counterparts. The Lax-Friedrichs method fails to produce accurate an accurate model for the behaviour of the system with a dx of 0.01. The Lax-Friedrichs produces a much more accurate model, but the system becomes unphysical at points (before drastic changes) and produces oscillations which do not exist in the real system. The HLL and HLLC on the other hand closely model the real system, only slightly deviating from the exact solution when drastic changes occur.

Question 1b



Figures 1 and 2: The density and pressure conditions for the the system after 0.012s. In this density graph the clear superiority of the HLLC can be seen, achieving a much more physical model.

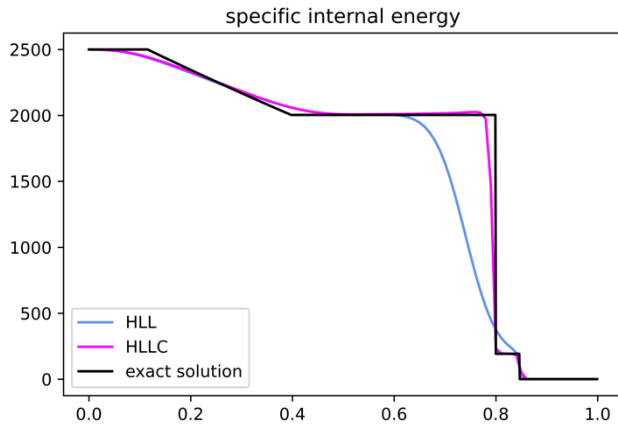


Figure 3: The specific internal energy data shock tube B. Again the HLLC solver achieves a simulation much closer to the exact data.

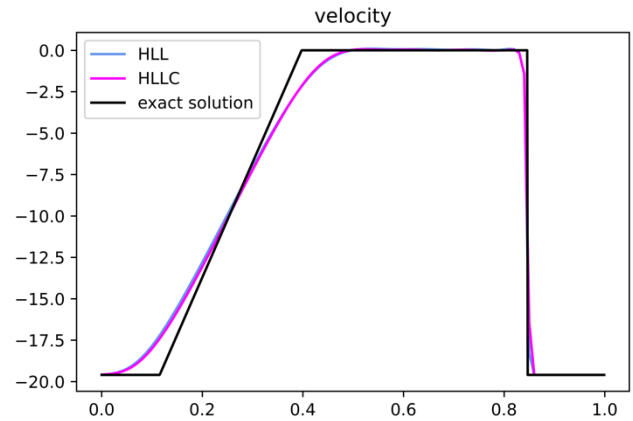


Figure 4: The velocity for shock tube B. Both the HLLC and HLL methods produce very similar results that are close to the exact solution.

In 1b the Lax-Wendroff method could not produce a model for shocktube B over the 0.012s time frame. This is due to the oscillations produced which can be seen in 1a. In 1b, these oscillations produced a negative density, which caused the solver to get stuck, as doing the square root of this would produce a NaN value. Although able to produce a solution, as seen above in 1a, both the HLLC and HLL solvers produced far superior solutions when simulating using a dx of 0.01. When comparing the HLL and HLLC solvers it was found that the HLLC produced results closer to the exact solution and thus was used moving forward.

The HLLC

As discussed earlier the HLLC was far superior to its counterparts in producing models very close to the exact data. Unlike the Lax-Wendroff, it also remains stable even with extreme starting conditions, as it does not produce the oscillations which cause problems with the Lax-Wendroff. As such it was used moving forward. The HLLC solver can be split up into 4 separate sections; setting the initial conditions, working out the sound speeds, the decision tree to calculate the correct half flux and the flux reconstruction algorithm.

The initial conditions were set based off the initial density, pressure and velocity data provided, which allowed the specific internal energy and total energy density of the fluid to be calculated. These were applied to each zone. Either side of the N zones being simulated a ghost cell was created in order to keep the boundaries constant. These would remain unchanged during the simulation.

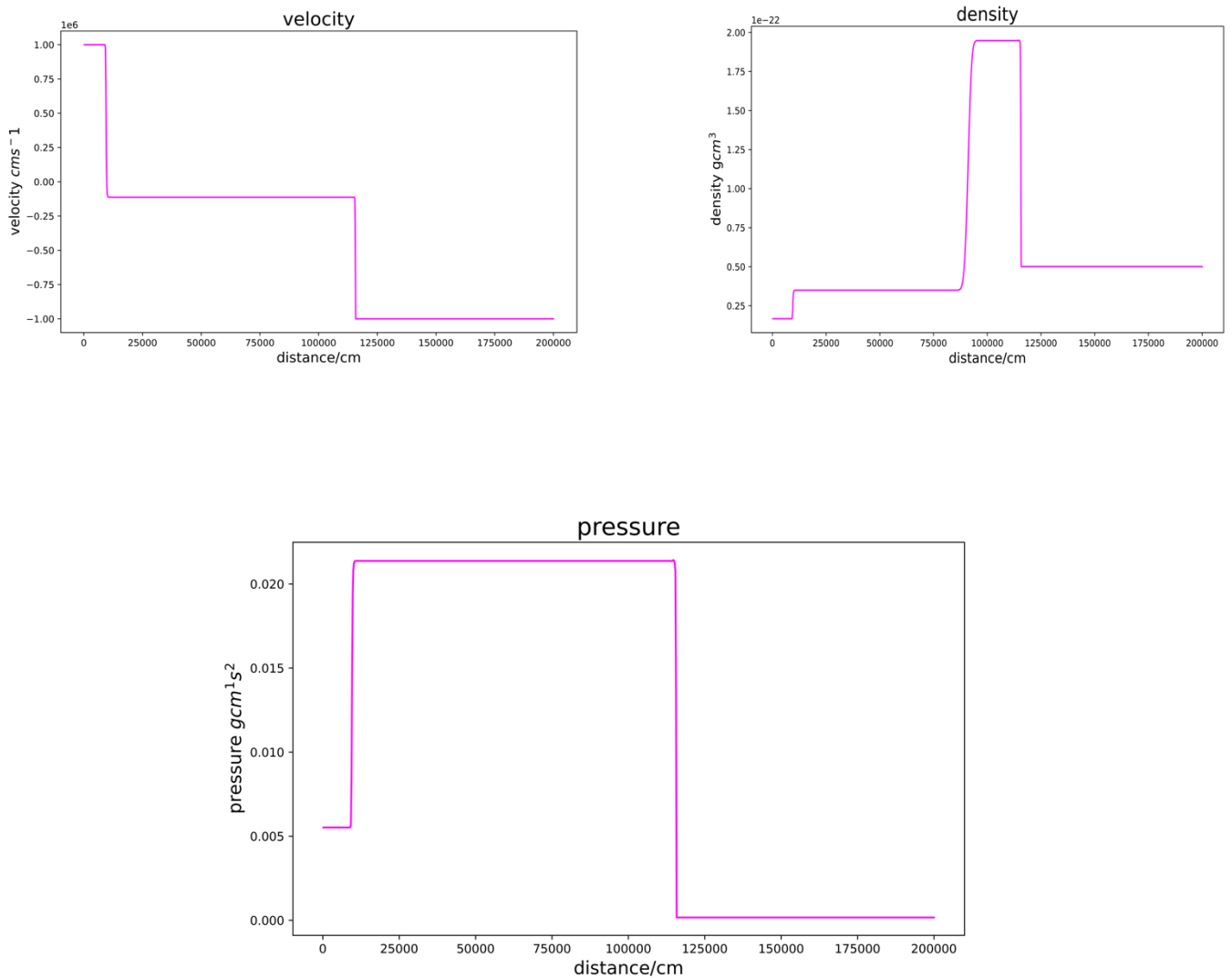
Once the initial conditions were set up, the main body of the solver exists within a while loop. If the current time remains below t_{max} , the simulation will continue. A for loop is then used to iterate across the whole distance being simulated, with the size of the step being equal to the zone size. In order to calculate the new fluid states, the initial cell fluxes

need to be calculated which in turn can be used to determine the fluxes between the cells. In order to achieve this the zone across the cell boundaries is split up into 4 sections. This is where the first decision tree is implemented. The pressure in the region between the waves is estimated which in turn are used to find an estimate for the speed of left and right moving waves in the fluid, depending on whether they can be classed as sub (sound wave) or supersonic (shock wave). If both waves are moving left, the intercell flux is equal the left cell, and if moving to the right the intercell flux is equal to the right cell. If the wave fronts are not travelling in the same direction, then they exist in the central or discontinuous zone. This zone is divided in two by the contact discontinuity, the speed of which is estimated from left and right wave speeds. Once the zones have been established, the fluxes in each zone can be determined, and the suitable flux for the half state calculated.

At this point the half fluxes for every zone boundary are known for this time step, and the flux reconstruction algorithm can be applied. This allows the new states to be calculated. It is at this point the time step is calculated from the Courant-Freidrichs-Lewis condition, such that the size of the time step is always less than the distance step divided by the maximum speed of the wave. The maximum speed of the wave in the grid frame is calculated by summing the absolute values of the gas and sound speed. The states and timestep can then be updated and if the time is still below t_{max} the process repeats.

Question 2

The HLLC solver was used for this simulation as discussed above, A Δx of 0.01 scale distance units was used in order to produce the 1000 zones required. The snapshots for the density, velocity and pressure were taken at a time of 0.08s. As is clear on all three graphs, this was when the shockwave approached the left boundary, as shown by the sharp rise in density at about 10000 cm. The slower moving right travelling wave can also be seen in the velocity and pressure graphs, by the sharp change at about 112500 cm. This most likely represents a sound wave, as shown by its much lower speed.



Figures 1, 2 and 3: The velocity/pressure/density-distance profile for the colliding gas clouds after a time of 0.08s. As in the previous 2 figures, the edge of the shockwave can be clearly seen at around $d = 10000\text{cm}$

